

ASSESSMENT IMPACT OF THE DAMIETTA HARBOUR (EGYPT) AND ITS DEEP NAVIGATION CHANNEL ON ADJACENT SHORELINES

Mohsen M. Ezzeldin¹, Osami S. Rageh², Mahmoud E. Saad³@

ABSTRACT:

Deep navigation channels have a great impact on adjacent beaches and crucial economic effects because of periodic dredging operations. The navigation channel of the Damietta harbour is considered a clear example of the sedimentation problem and deeply affects the Northeastern shoreline of the Nile Delta in Egypt. The aim of the present study is to monitor shoreline using remote sensing techniques to evaluate the effect of Damietta harbour and its navigation channel on the shoreline for the last 45 years. Also, the selected period was divided into two periods to illustrate the effect of man-made interventions on the shoreline. Shorelines were extracted from satellite images and then the Digital Shoreline Analysis System (DSAS) was used to estimate accurate rates of shoreline changes and predict future shorelines evolution of 2030, 2040, 2050 and 2060. The Damietta harbour created an accretion area in the western side with an average rate of 2.13 m year⁻¹. On the contrary, the shoreline in the eastern side of the harbour retreated by 92 m on average over the last 45 years. So, it is considered one of the main hazard areas along the Northeastern shoreline of the Nile Delta that needs a sustainable solution. Moreover, a detached breakwaters system is predicted to provide shore stabilization at the eastern side as the implemented one at Ras El-Bar beach. Predicted shoreline evolution of 2060 shows a significant retreat of 280.0 m on average.

Keywords: Navigation Channel; Shoreline; Damietta Harbour; Remote Sensing; DSAS.

RESUMO:

Os canais de navegação profundos têm um grande impacto nas praias adjacentes e efeitos econômicos cruciais devido às operações de dragagem periódicas. O canal de navegação do porto de Damietta é considerado um exemplo claro do problema de sedimentação e afeta profundamente a costa nordeste do Delta do Nilo, no Egito. O objetivo do presente estudo é monitorar a linha costeira usando técnicas de sensoriamento remoto para avaliar o efeito do porto de Damietta e seu canal de navegação na linha costeira nos últimos 45 anos. Além disso, o período selecionado foi dividido em dois períodos para ilustrar o efeito das intervenções feitas pelo homem na costa. As linhas costeiras foram extraídas de imagens de satélite e, em seguida, o Digital Shoreline Analysis System (DSAS) foi usado para estimar taxas precisas de mudanças na linha costeira e prever a evolução futura das linhas costeiras em 2030, 2040, 2050 e 2060. O porto de Damietta criou uma área de acreção no lado oeste com uma taxa média de 2.13 m ano⁻¹. Em contrapartida, a linha da costa no lado oriental do porto recuou 92 m em média nos últimos 45 anos. Portanto, é considerada uma das principais áreas de risco ao longo da costa nordeste do Delta do Nilo que precisa de uma solução sustentável. Além disso, um sistema de quebra-mares isolado está previsto para fornecer estabilização da costa no lado leste como o implementado na praia de Ras El-Bar. A evolução da linha costeira prevista para 2060 mostra um recuo significativo de 280 m em média.

Palavras-chave: Canal de navegação; Costa; Porto de Damietta; Sensoriamento remoto; DSAS.

1 Irrigation and Hydraulics Department, Faculty of Engineering, Mansoura University, Mansoura 35516, Egypt. Email: mohsen-ezzeldin@hotmail.com

2 Irrigation and Hydraulics Department, Faculty of Engineering, Mansoura University, Mansoura 35516, Egypt. Email: drosamirageh@yahoo.com

3 Irrigation and Hydraulics Department, Faculty of Engineering, Mansoura University, Mansoura 35516, Egypt. Corresponding author: miskver@yahoo.com

@ Corresponding author: miskver@yahoo.com

1. INTRODUCTION

Navigation channels are a determined path dredged in the sea bed to enable ships to access harbours or to pass through countries. The channel extends from port location to the required water depth in the sea, where depth and width of the channel depend on the ship dimensions. Navigation channels usually act as sediment traps and interrupt sediment movement from various directions due to waves and currents. Sedimentation happens when suspended load reaches the channel location with bigger water depth and low current velocity. Hence, construction of deep navigation channels usually affects the contiguous beaches, because of losing suspended material that is trapped in navigation channels.

In deep navigation channels, periodic dredging is usually needed to ensure the safe passage of vessels and maintain the water depth of navigation channel at the required level, but the volume of dredged material varies from a location to another. In Argentina, El-Toro navigation channel required periodic dredging to remove 300 000 m³year⁻¹ of sediment (Perillo and Cuadrado, 1991). In Thailand, the approach channel of Bangkok harbour is maintained through continuous dredging of 5 million m³year⁻¹ of sediment (Deguchi *et al.*, 1994). Moreover, the entrance channel at Blankenberge harbour, Belgium, had a total amount of sediment of 165 000 m³year⁻¹ (Zimmermann *et al.*, 2012) and the estimated rate of sediment in the navigation channel of LNG port at Abu-Qir bay on the northwestern coast of Nile Delta, Egypt, was 1 977 000 m³year⁻¹ (Deabes, 2010). Furthermore, the international navigation channel in Dinh An Estuary, Vietnam, used to be dredged twice a year, where siltation volume reached 1 250 000 m³year⁻¹ (Nguyen *et al.*, 2013), and the average rate of siltation in Saint John harbor, Canada, was 4 200 000 m³year⁻¹ (Leys *et al.*, 2011). Also, the navigation channel at Damietta port trapped longshore sediment and gained sedimentation with an average rate of 2 000 000 m³ year⁻¹ (Frihy *et al.*, 2016).

Dredging activities in navigation channels and man-made interventions in the coastal system contribute to the erosion of the adjacent beaches (Da Silveira *et al.*, 2012). Changing the alignment and depth of the navigation channel at Dar el Sallam harbor, Tanzania, caused high erosion in Ras Makabe and the sedimentation rate increased to 168 000 m³year⁻¹ (Sanga and Dubi, 2004). So, the construction of a deep navigation channel has clear environmental effects on the adjacent shoreline.

The shoreline is the interface between sea and land and represents one of the main natural borders for many countries,

and can be used for tourism, recreation activities, urbanization and industrial and infrastructures activities. Assessment and analysis of shoreline changes are very important in coastal area management, understanding of morphological processes, computing sediment budget and identification of hazard zones (Danforth and Thieler, 1992). Monitoring shoreline changes can be used to illustrate for instance the environmental effect of navigation channels on adjacent beaches. Also, an erosion/accretion pattern reveals the natural processes of wave-induced longshore current and sediment transport (El Banna and Herehe, 2009).

From 1807 to 1927 ground surveying was the only way used for shoreline mapping. Aerial photographs were used for that purpose in the period from 1927 to 1980, and then from 1972 Landsat and other satellites provide digital imagery in infrared spectral bands that facilitate monitoring operations. Using satellite images in shoreline monitoring has many advantages since optical images are simple to interpret and easily obtainable. In addition, absorption of infrared wavelength region by the water make such images an ideal combination for mapping. Besides, it is not time-consuming, inexpensive to implement and it has large ground coverage.

Landsat images were used in shoreline monitoring in the last decades to evaluate shoreline response to coastal structures and determine accretion and erosion pattern. El Banna and Hereher (2009) used satellite images for analyzing the coast of Sini, Egypt, in the period between 1986 and 2001. Dewidar and Frihy (2010) used ten scenes of Landsat satellite images for 35 years from 1972 to 2007 to quantify erosion and accretion along Northeastern shoreline of Nile delta in Egypt. El-Sharnouby *et al.* (2015) used ten Landsat images for monitoring shoreline changes of Gamasa beach, Egypt, with 30 km length over 30 years. Moreover, the impact of port construction, siltation, land reclamation and urban development on Ningbo shoreline, China was evaluated by seven Landsat images for 40 years from 1976 to 2016 (Wang *et al.* 2017). Also, the rates of change of the North-Holland coast, Netherlands, were estimated by 13 Landsat images from 1985 to 2010 (Do *et al.* 2019). El nabwy *et al.* (2020) used eight Landsat satellite images for 33 years from 1985 to 2018 to estimate the shoreline changes in the northeast shoreline of the Nile Delta, Egypt, and the effect of the seawalls on it.

The Northern coastline of the Delta in Egypt has suffered from erosion in many spots in the last decades due to blockage of sediment discharge as a consequence of the Aswan High

Dam construction and constructed barrages across Nile River. Damietta harbour and its navigation channel are considered a clear example of sedimentation problem and impacts on adjacent beaches.

El-Asmar and White (2002) used remote sensing and field survey to assess shoreline changes consequent to harbour construction from 1983 to 1993. It was found that harbour jetties interrupted eastward-moving littoral drift. Therefore, the western beach had accretion of fine sand with an average rate of 25 m year⁻¹ from 1983 to 1993. In contrast, the eastern shoreline was losing coarse sand that was trapped in the navigation channel and the erosion rate reached -26 m year⁻¹. Frihy *et al.* (2004) evaluated the construction of large-scale detached breakwater systems on the Nile Delta coast of Egypt at Ras El Bar beach with a monitoring program spanning the years 1990 to 2002 and beach nearshore profiles. The preconstruction beach erosion at Ras El Bar (-6 m year⁻¹) was replaced by the formation of a sand tombolo (35 m year⁻¹) and salient (9 m year⁻¹). On the other hand, beach erosion substantially increased in the downdrift sides and reached -9 m year⁻¹.

Abo Zed (2007) used 18 bathymetric profiles to study the erosion/accretion pattern before the construction of Damietta harbour (1978-1982) and after the construction (1988 - 1997). The area was marked as an accretion zone before construction of harbour and then after the construction, it was observed that there was an accretion zone in the western side and an erosion zone in the eastern side of the harbour. The annual net rate of littoral drift on the western side was about 143 000 m³ (accretion) and on the eastern side was about 254 000 m³ (erosion).

El-Asmar *et al.* (2016) used 5 scenes from 1973 to 2015 to monitor the shoreline in the eastern side of Damietta harbour, that was an erosive segment with high shoreline retreat. Khalifa *et al.* (2017) used 32 bathymetric profiles to evaluate shoreline changes in the surrounding area of Damietta harbour from 2010 to 2015. The data revealed an accretion zone in the western side with an average rate of 15 m year⁻¹ and erosion pattern at eastern part with an average rate of - 6.5 m year⁻¹.

Previous literature proves that man-made interventions such as the construction of dams, deep navigation channels and breakwaters deeply affect shoreline morphology.

This research aims to evaluate the impact of harbours and deep navigation channels on neighboring beaches. Damietta harbour with deep channel could be a good example and case study for this purpose. The rate of shoreline change needs to

be updated and estimated using high precision and accurate method. Furthermore, prediction of future shoreline could clarify the effect of the harbour on the shoreline in the next decades. Remote sensing technique was used in shoreline monitoring and then, DSAS was used to determine the rates of shoreline change using statistical approaches.

2. THE CASE STUDY OF THE DAMIETTA HARBOUR

2.1. Introduction

In the 1980s, the Egyptian authority decided to establish the Damietta harbour on the northeastern side of the Nile Delta near the New Damietta city to improve trade and economy potential along the Mediterranean Sea. The selected location 9.7 km west of the Damietta Nile branch is characterized by a minimum wave and current effect. However, the location was described as one of long-term coastal accretion area (El-Asmar and White, 2002).

In 1982, the breakwaters of Damietta harbour were constructed to protect the harbour entrance from siltation. The western breakwater was constructed parallel to the navigation channel with 1500 m length and extends to 7.0 m water depth and the eastern breakwater was constructed perpendicular to the shoreline with 500 m length and extends to 3.0 m water depth. The navigation channel was completed in 1984, with a total length of 20 km, 15 m average water depth and 200 m width of the inner part that increases to 300 m in the outer part (Figure 1).

As a result of the harbour construction, the shoreline in the eastern side suffered erosion and Ras El-Bar beach began to retreat, threatening tourism and recreational activities. So, from 1991 to 2002, a detached breakwater system consisting of eight breakwaters was constructed in Ras El-bar area to protect the shoreline. Breakwaters are 200 m long with 200 m gaps between each other and were constructed 400 m offshore at 4.0 m water depth.

2.2. Study area description

The study area is the shoreline around Damietta harbour with a total length of 26.2 km, and it was divided into three zones (Figure 2). Zone A extends from Gamasa drain to the western breakwater of Damietta Harbour with a length of 18.50 km. Zone B extends from the eastern breakwater to the location of detached breakwaters with a length of 4.5 km. Zone C extends beyond the detached breakwaters of Ras El-Bar beach with a length of 3.2 km. The aim of the present study is to monitor



Figure 1. Layout of Damietta harbour.

shoreline changes to evaluate the effect of Damietta harbour and its navigation channel on the shoreline for the last 45 years. The selected period was divided into two periods, the first period was from 1973 to 1994 to analyze the changes in shoreline before and after Damietta harbour construction and before the construction of shore protection structures. The second period was from 1995 to 2018 and it illustrates shoreline changes after the construction of detached breakwaters at zone C.

2.3. Meteorological analysis

Coastal processes depend on meteorological factors such as wind, waves, tide, and current. So, analysis of the metrological data is very important for the assessment of coastal changes. The predominant wind direction at northeastern coast of Nile Delta is between N and NW direction with an average wind speed of about 3.75 m s^{-1} (Khalifa, 2017).

According to records from 2001 to 2004, the predominant waves in the Damietta harbour come from NW direction (76.8%) and a small portion of waves comes from NE direction (13.6 %) and other waves come from SE (5.3%) and SW (4.3%), Figure 3. The maximum wave height was 4.8 m with significant wave

height and a period of 1.10 m and 6.7 s, respectively. Collected data was measured by Coastal Research Institute (CoRI) and Hydraulic Research Institute (HRI), Egypt. It is obvious that, the prevailing wave direction is NW and it is responsible for generating net longshore sediment transport from west to east. However, a reverse current is generated toward SW direction in winter seasons with an average velocity of 0.30 m s^{-1} . Also, referring to the measurement of water surface elevations, the North-eastern shoreline of Nile Delta has semidiurnal tide and maximum tidal range (H.H.W.L - L.L.W.L) is about 0.75 m.

From the previous analysis, it is obvious that sediment flux is transporting in both directions from west to east and from east to west, due to currents and waves. So, N-E orientation of the navigation channel interrupts moving littoral drift from both directions and affects the shoreline in both western and eastern sides.

3. MATERIALS AND METHODS

The monitoring program followed many steps such as data acquisition, shoreline extraction and shoreline analysis, analyze

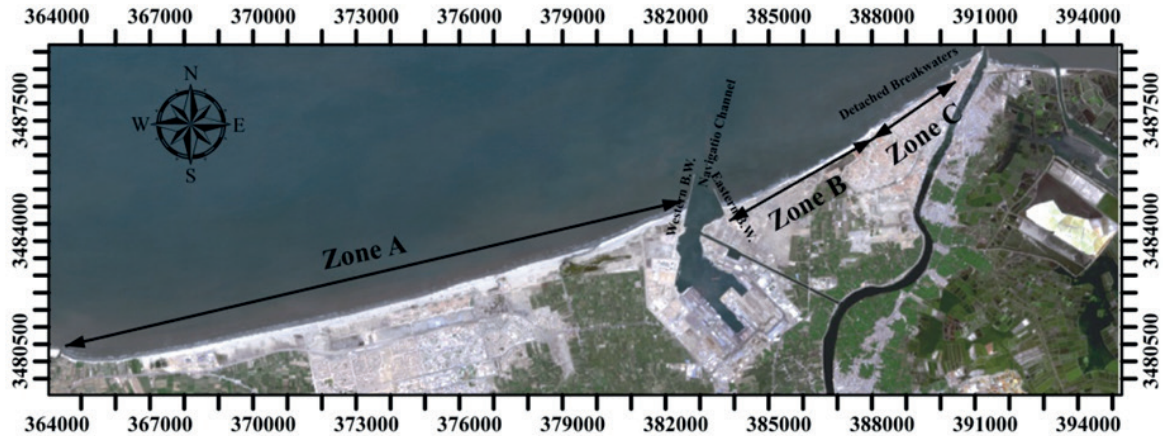


Figure 2. Study Area Zones.

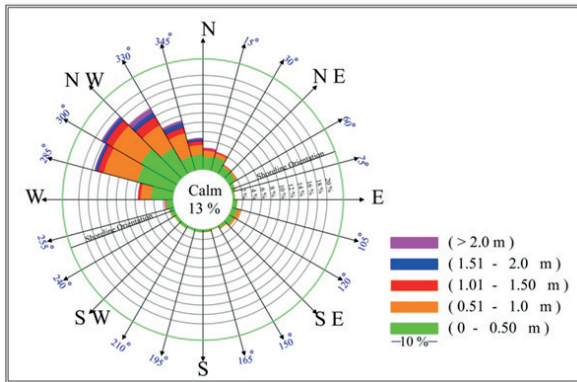


Figure 3. Wave Rose at Damietta harbor.

shoreline changes, determination of hazard areas among the study area and prediction of future shorelines (Figure 4).

3.1. Data acquisition

Satellite images were acquired from earth explores sites maintained by United States Geological Survey (USGS) and from Landsat satellite dataset. Landsat images were acquired in unequal intervals to ensure data acquisition in good weather condition with low cloud cover to reduce the error due to variability of shoreline position and minimize the influence of the tide (Moore, 2000). Table 1 illustrates scenes properties such as date, satellite name, sensor type and image resolution.

3.2. Image processing

Acquired images were subjected to image processing such as geometric correction, radiometric correction and atmospheric correction using ENVI V5.30 software. Geometric correction is performed to eliminate distortion related to scale variation, tilt

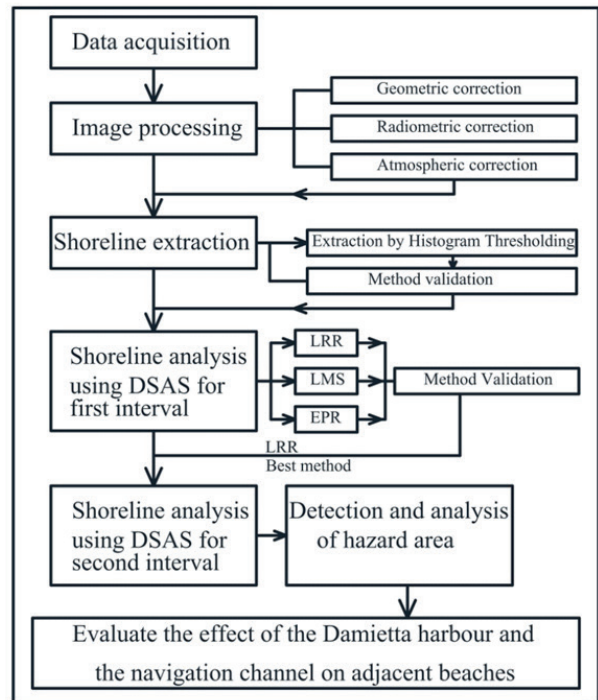


Figure 4. Flowchart of the monitoring program.

and lens distortion, and it is carried out from Ground Control Points (GPCs). Satellite images were geometrically rectified to the Universal Transverse Mercator (UTM) with a spheroid and datum of WGS 84, Zone 36. Radiometric calibration means a conversion of recorded DN values (0-255) to at-surface reflectance. Atmospheric correction is removing the effects of the atmosphere to produce surface reflectance values and can significantly improve the interpretability and use of an image.

Table 1. Satellite images properties.

Period	Acquisition Date	Satellite	Acquisition Time	Water Level (m)	Sensor Type	Scene Path/row	Spatial Resolution (m)
I	1973-01-04	Landsat 1	8:00	0.65	MSS	190/038	60.0
	1978-05-20	Landsat 3	7:47	0.53	MSS	190/038	60.0
	1984-04-29	Landsat 5	7:50	0.65	TM	176 / 038	30.0
	1987-03-21	Landsat 5	7:45	0.39	TM	176 / 038	30.0
	1990-03-29	Landsat 5	7:43	0.24	TM	176 / 038	30.0
	1992-04-03	Landsat 5	7:47	0.57	TM	176 / 038	30.0
	1994-04-09	Landsat 5	7:43	0.60	TM	176 / 038	30.0
II	1995-03-11	Landsat 5	7:33	0.51	TM	176 / 038	30.0
	2000-11-11	Landsat7	8:13	0.82	ETM	176 / 038	30.0
	2005-05-25	Landsat 5	8:10	0.52	TM	176 / 038	30.0
	2010-04-05	Landsat 5	8:14	0.54	TM	176 / 038	30.0
	2013-04-13	Landsat 8	8:25	0.37	OLI/TIRS	176 / 038	15.0
	2016-03-04	Landsat 8	8:23	0.55	OLI/TIRS	176 / 038	15.0
	2018-03-26	Landsat 8	8:22	0.60	OLI/TIRS	176 / 038	15.0

3.3. Shoreline extraction

There are different methods for shoreline extraction from satellite images. Histogram thresholding on one of the infrared bands is widely used method in shoreline delineation since the reflectance of water is nearly equal to zero and reflectance of land is greater than water. For example, band 5 is the best for extracting land-water interface in case of TM or ETM satellite images (Niya *et al.*, 2013, Alesheikh *et al.*, 2007). After the image processing, final binary images were obtained and were processed in ArcGIS10.2 software to extract the shoreline. Each image was converted from raster to vector to obtain the clear interface between land and water as the shoreline. Figure 5 shows sample of the extracted shoreline over the period of study.

3.4. Uncertainty in of shoreline change

Using satellite images in the analysis of shoreline changes has a range of error. The source of error may be due to geo-referencing error and short-term variability of shoreline position, (Louati *et al.*, 2015, Kumar *et al.* 2010). For the selected satellite images the RMSE in geo-referencing process did not exceed 0.6 pixels, that is considered an acceptable error (Kabir *et al.* 2020). So, the maximum geo-referencing error is ± 28.5 m for the period (1973-1984), ± 9.4 m for the period (1984-2013) and ± 7.5 m for the period (2013-2018). On the other hand, most of Landsat scenes were acquired in spring period and during calm sea condition that tidal ranging 0.1 to 0.50

m. Hence, the predicted shift in shoreline position varies from movement ± 2.50 m to ± 12.5 m according to the beach slope. Regarding the spatial resolution of Landsat images that varied from 60×60 m, 30×30 m and 15×15 m, the Landsat images could be used in analysis of shoreline changes neglecting the tidal effect (Louati *et al.*, 2015; El-Sharnouby *et al.* 2015; Kuleli, 2010; Dewidar and Frihy 2007; Guariglia *et al.* 2006). So, the total error based on geo-referencing error is ± 3.86 m, ± 1.01 m, ± 3.06 m and ± 0.97 m for the period (1973-1984), (1984-2013), (2013-2018) and (1973-2018) respectively.

3.5. Validation of Shoreline Extraction Method

To validate the shoreline extraction method and determine its accuracy, the extracted shoreline from the satellite image of 2013 was compared with another shoreline that was generated by a field survey for the same year. The comparison between shorelines was carried out by the Digital Shoreline Analysis System (DSAS) using a statistical approach of End Point Rate (EPR). Results showed a good agreement between the extracted shoreline from the satellite image and that from the field survey with Mean Absolute Error (MAE) of 6.3 m (Figure 6.a). Figure 6.b shows that 90 % of the values have small errors ranging between -5 and +15 m (20 m). The error may be because of geo-referencing process or short-term variability of shoreline position, however it can be considered an acceptable error according to the used the pixel size of the satellite image (15.0 m) (Wang *et al.* 2017).

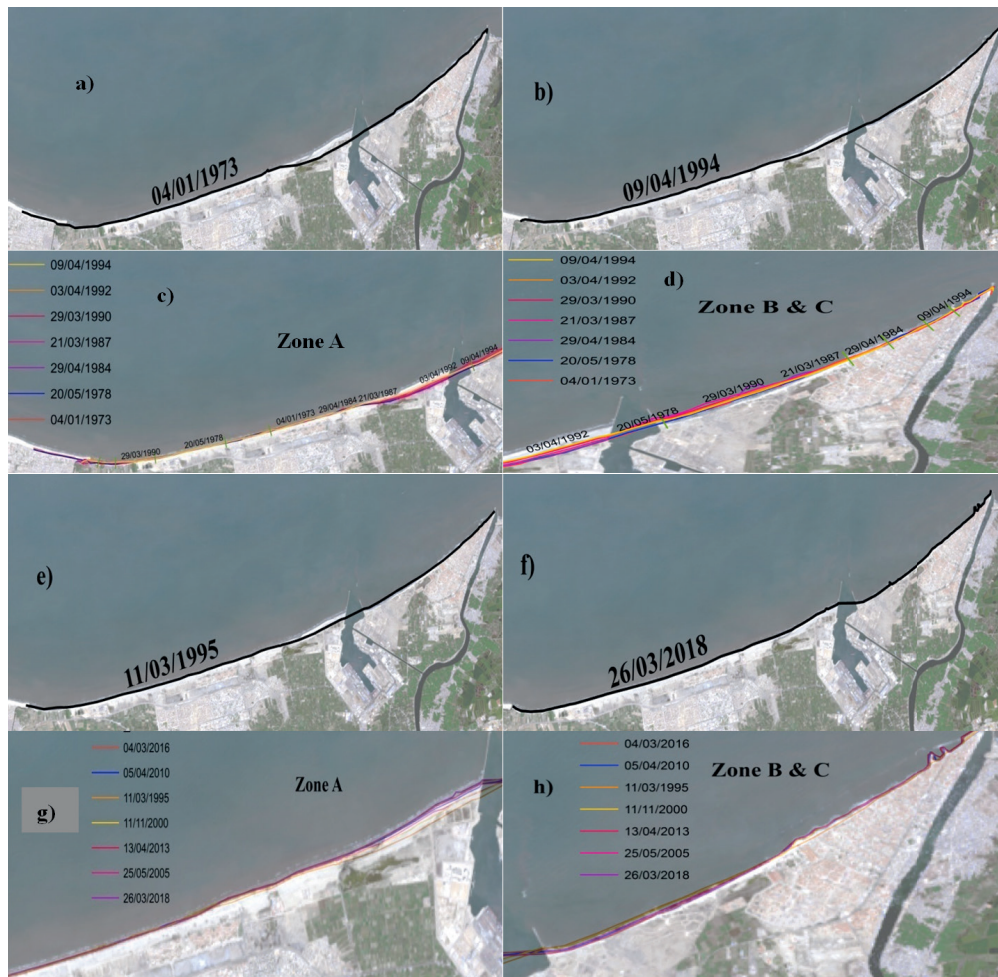


Figure 5. a,b) Satellite images for the two years 1973 and 1994, c) Extracted shorelines for the first period (1973–1994) For zone A, d) Extracted shorelines for the same period for zone B and C e,f) Satellite images for the two years 1995 and 2018, g) Extracted shorelines for the second period (1995–2018) for zone A, h) Extracted shorelines for the same period for zone B&C.

3.6. Shoreline analysis using DSAS

DSAS is a software extension within the Environmental System Research Institute (ESRI) ArcGIS. DSAS can be used in the analysis of shoreline changes, computing erosion/accretion rates over historical timescales and prediction of the shoreline evolution as an indicator of future trend assuming constant physical nature. Different statistical approaches such as End Point Rate (EPR), Linear Regression Rate (LRR) and Least Median of Squares (LMS) were used in the calculations. Shorelines are merged into one feature class to perform statistical analysis. Transects with 10 m spacing, were generated perpendicular to this baseline and intersected the shorelines to establish measurement points. Statistical approaches were used to calculate the average rate of shoreline changes.

4. ANALYSIS OF RESULTS AND DISCUSSION

4.1. First period (1973 – 1994)

Statistical methods of EPR, LRR and LMS were used to calculate the rates of change in both study periods. Table 2 summarizes the results and the rates of change for each zone for the first period.

Also, Figure 7 shows the variable rates of shoreline change along the study area using the different methods.

To validate the statistical results and determine the most accurate method in calculating shoreline rates of change, the results from statistical calculations were compared with other results that were generated from field ground survey by Frihy and Komar (1993) at the same locations (Figure 8). Frihy and

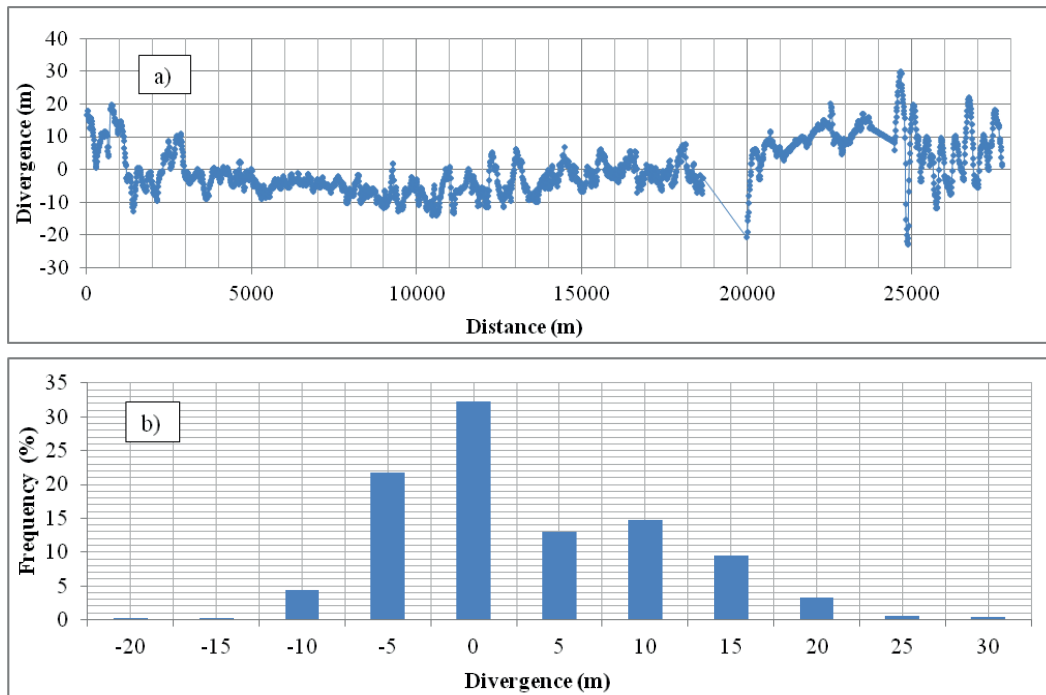


Figure 6. a) Differences between shoreline from satellite image and field survey, b) Frequency for each divergence value.

Table 2. Summary of statistical results for the first period (1978 – 1994)

Zone	Total Length (km)	Transect Lines	Average Rates of Change (m/year)			Zone Description	Net Shore Movement (NSM) (m)		
			EPR (m year ⁻¹)	LMS (m year ⁻¹)	LRR (m year ⁻¹)		Max.	Min.	Average
A	18.50	1822	1.50	3.08	1.95	Accretion	+ 179.8	+ 0.09	+ 75.0
B	4.50	426	0.32	-4.98	1.98	Accretion	+ 83.7	+0.09	+ 32.70
C	3.20	282	-1.35	-0.68	-1.20	Erosion	- 74.36	-1.84	- 36.27
Total	26.20	2530							

Komar (1993) used 65 beach profiles along 240 km of the Delta coastline that has been obtained annually from 1971 to 1990. Profile lines were perpendicular to shoreline that were spaced by 0.5 to 10 km and extend to a water depth of 6 m.

Table 3 shows a comparison between estimated rates from DSAS and computed rates from the field survey profiles at certain locations. It seems that, both EPR and LRR methods give better results (Figure 9), with correlation coefficients of 0.60 and 0.58, respectively. Although LRR had lower correlation coefficient than EPR, it will be used in calculations as it uses all data points in the rate calculation to reduce the influence of spurious data counter to EPR method.

LRR results show that zone A includes an accretion area representing 65 % of the total zone and characterized by a variable change rate from 0 to 9.22 m year⁻¹ with an average annual rate of 3.44 m year⁻¹, and another erosion area representing 35 % of the total zone with change rate ranging between 0 and -4.72 m year⁻¹ and an average annual rate of -0.90 m year⁻¹ (Figure 10). However, Zone A can be considered generally an accretion zone since shoreline stepped forward by 75.0 m in average and an average annual rate of change of +1.95 m year⁻¹. Zone B is also considered an accretion zone (with a small erosion zone corresponding to 18% of zone B) with a maximum accretion rate of 6 m year⁻¹ and an average rate of change of +1.98 m year⁻¹. Zone B was used as a dumping

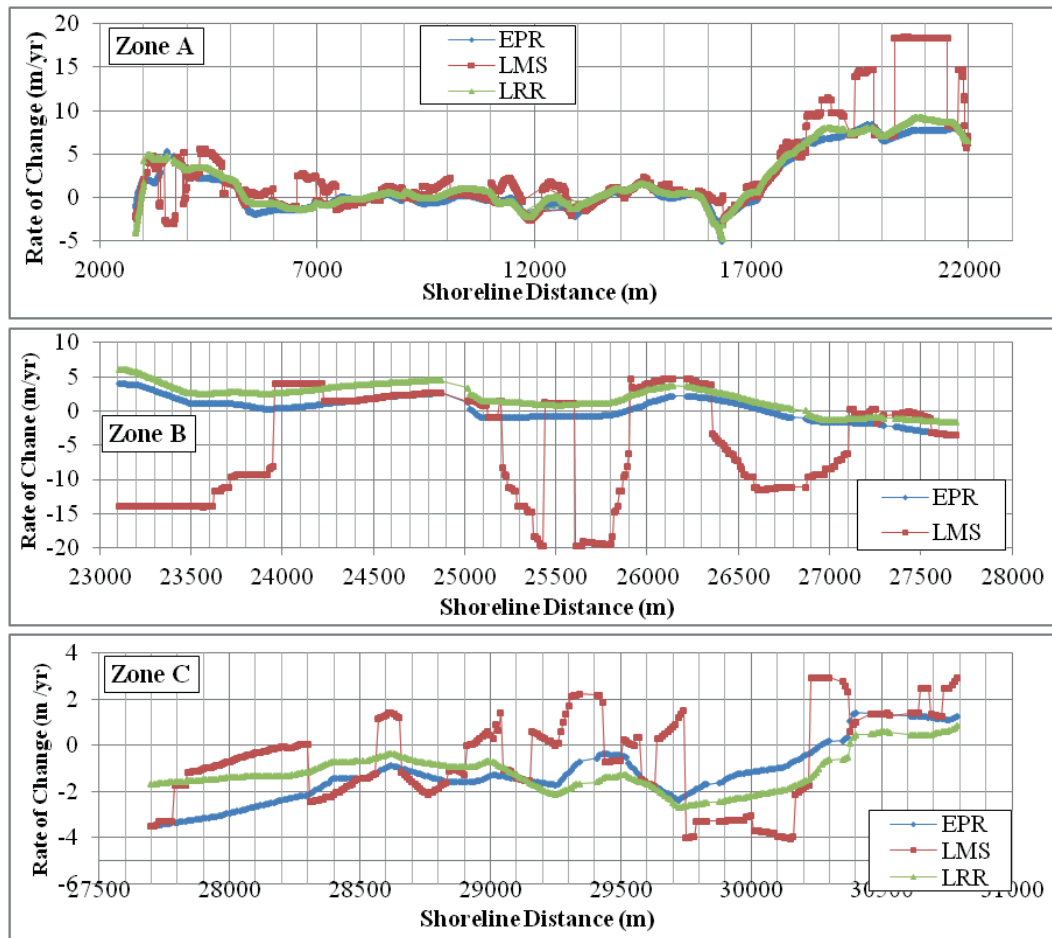


Figure 7. The rates of shoreline change using different methods for the first period (1978 - 1994).

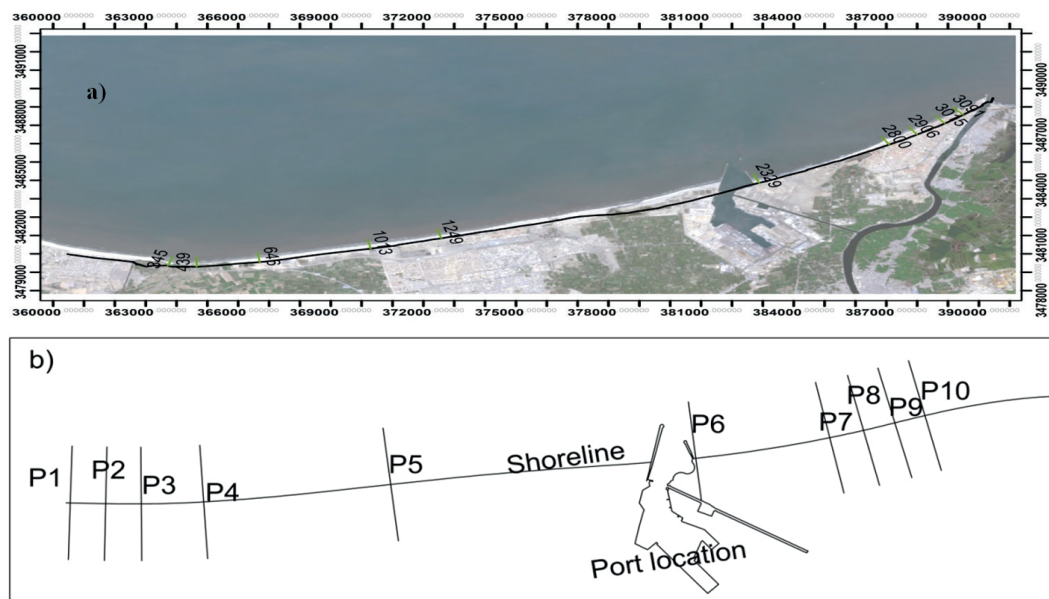


Figure 8. a) Location of transects used in the statistical analysis in the present study, b) Profile numbers and location of survey profiles by Frihy and Komar, (1993).

Table 3. The comparison between DSAS results and field survey results.

Present Study			The annual rate of shoreline change (m/year)				Frihy and Komar (1993)		
Transect ID	Location		No. Profile Location				East (UTM)	North (UTM)	
	East (UTM)	North (UTM)	DSAS Results			Ground Survey			
			EPR	LMS	LRR				
345	363795.2	3479581	4.18	4.29	4.33	5.8	P1	363743.1	3479671
439	364650.3	3479545	2.22	5.19	3.46	3.2	P2	364662.2	3479649
646	366662.2	3479801	-1.36	-1.11	-1.26	2.2	P3	366687.4	3479860
1013	370241.8	3480528	-0.02	0.35	0.77	0.9	P4	370207.9	3480584
1249	372513.1	3481085	-0.79	1.24	0.02	-1.2	P5	372571.3	3481104
2329	382790.4	3484094	3.18	-13.92	4.84	1.2	P6	382762.1	3484184
2800	386972.5	3486162	-2.97	-0.75	-1.4	0.3	P7	387019.2	3486278
2906	387863.6	3486702	-1.35	-1.07	-0.99	-0.1	P8	387937.8	3486786
3015	388753.3	3487301	-0.86	-4.02	-1.89	-0.2	P9	388812.6	3487380
3091	389341.4	3487764	1.88	1.88	1.8	-0.6	P10	389493.4	3487997
Correlation coefficient			0.60	0.30	0.58				

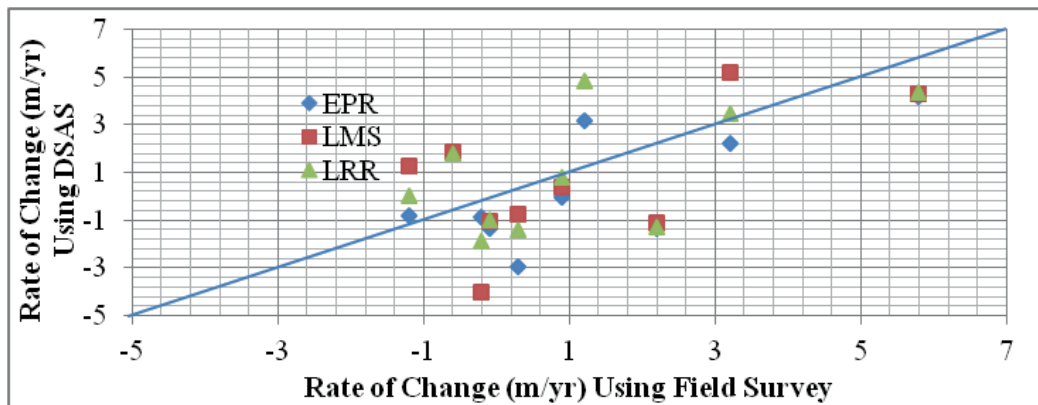


Figure 9. Validation of statistical results of the present study with ground survey results by Frihy and Komar (1993).

area of the dredged material from the navigation channel. So, the accretion rate of this zone after the harbour construction is related to the nourishment with the dredged material. The selection of this site to dump the dredged materials was not the best solution because the southwesterly reverse currents redistributed the dredged material and carried it back to the navigation channel. So, authorities changed the dumping site and decided to use the dredged material in recovering eroded beaches. On the contrary, zone C suffered from erosion that reached -2.7 m year^{-1} with an average rate of $-1.20 \text{ m year}^{-1}$ and the shoreline retreated with -74 m in some locations and -36.2 m on average. So, Egyptian authorities adopted a shore

protection project composed of detached breakwaters in zone C to protect the valuable shoreline of Ras El-Bar.

4.2 Second period (1995 – 2018)

According to DSAS results, zone A followed the same trend in the second interval and 70 % of the area was under accretion and with change rates varying from 0 to $11.88 \text{ m year}^{-1}$ with an average annual rate of 3.78 m year^{-1} , where 30 % of the zone has erosion with variable rate that ranging from 0 to -5.3 m year^{-1} and an average rate of $-1.64 \text{ m year}^{-1}$. So, zone A is still considered generally an accretion zone with an average annual rate of change of $+2.13 \text{ m year}^{-1}$ and the shoreline had

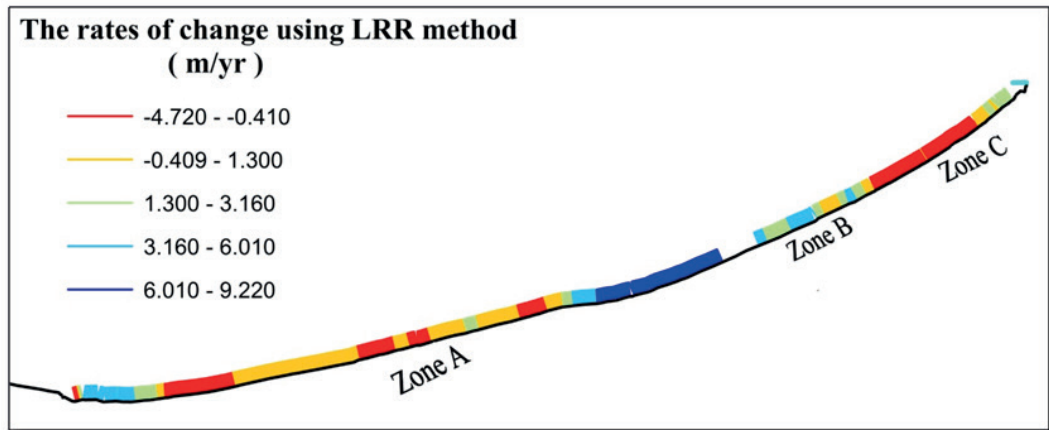


Figure 10. The rates of shoreline change using LRR method for the First period (1978 – 1994).

Table 4. Summary of statistical results for the second period (1995 – 2018).

Zone	Total Length (km)	Transect Lines	Average Rate of Change (m year ⁻¹)			Zone Description	Net Shore Movement NSM (m)		
			EPR (m/ year)	LMS (m/ year)	LRR (m/ year)		Max.	Min.	Average
A	18.50	1817	2.67	1.12	2.13	Accretion	+ 293.80	+ 0.06	+ 85.70
B	4.50	413	-4.26	-3.96	-4.30	Erosion	- 143.56	- 11.10	- 98.40
C	3.20	299	2.26	-0.17	1.81	Accretion	+ 106.8	+ 0.16	+ 56.30
Total	26.20	2529							

an average progressive of 85.70 m. On the other side, zone B was converted to erosion zone with a change rate ranging from 0 to -6.6 m year⁻¹ and an average of -4.30 m year⁻¹. In addition, shoreline retreated 143.5 m in some points with an average regressive of -98.40 m. On the other hand, in zone C as a result of the implemented detached breakwaters, the erosion rate changed to an accretion rate varying from 0 to 3.97 m year⁻¹ with an average value of + 1.81 m year⁻¹ and the shoreline stepped forward 106.8 m in some points and 56.30 m in average. Table 4 summarizes the results for each zone.

Figure 11 also shows the variable rates of shoreline change along the study area using LRR method for each zone.

From the data analyzed, it can be concluded that the construction of the Damietta harbour significantly impacted the adjacent shoreline, increasing the accretion rate in zone A with 10 %, Figure 12. The western breakwater of the harbour blocks the littoral drift from the west and accumulated sand generating an accretion zone on the western side. However, Zone B was converted from an accretion zone to an erosion zone with a high

erosion rate as the western breakwater of the harbour and the navigation channel block the littoral drift moving toward the east. On the other hand, the implemented detached breakwaters at Zone C showed a good performance since the erosion problem was solved and the shoreline was improved with an average rate of 1.81 m year⁻¹.

Therefore, zone B is considered to be one of the main hazard areas along the Northeastern shoreline of Nile Delta and needs a comprehensive and intensive study to determine the proper solution for this area.

4.3 Analysis of hazard area

Damietta harbour has a deep effect on zone B leading to high erosion rate. The area was analyzed with DSAS to measure the change in the total period from 1973 to 2018, Figure 13. The average rate of change varies from -4.64 m year⁻¹ to -1.16 m year⁻¹ with an average value of -3.39 m year⁻¹. Also, NSM shows that the shoreline retreated from 1978 to 2018 by 156.3 m in some points and 92 m on average, Figure 14.

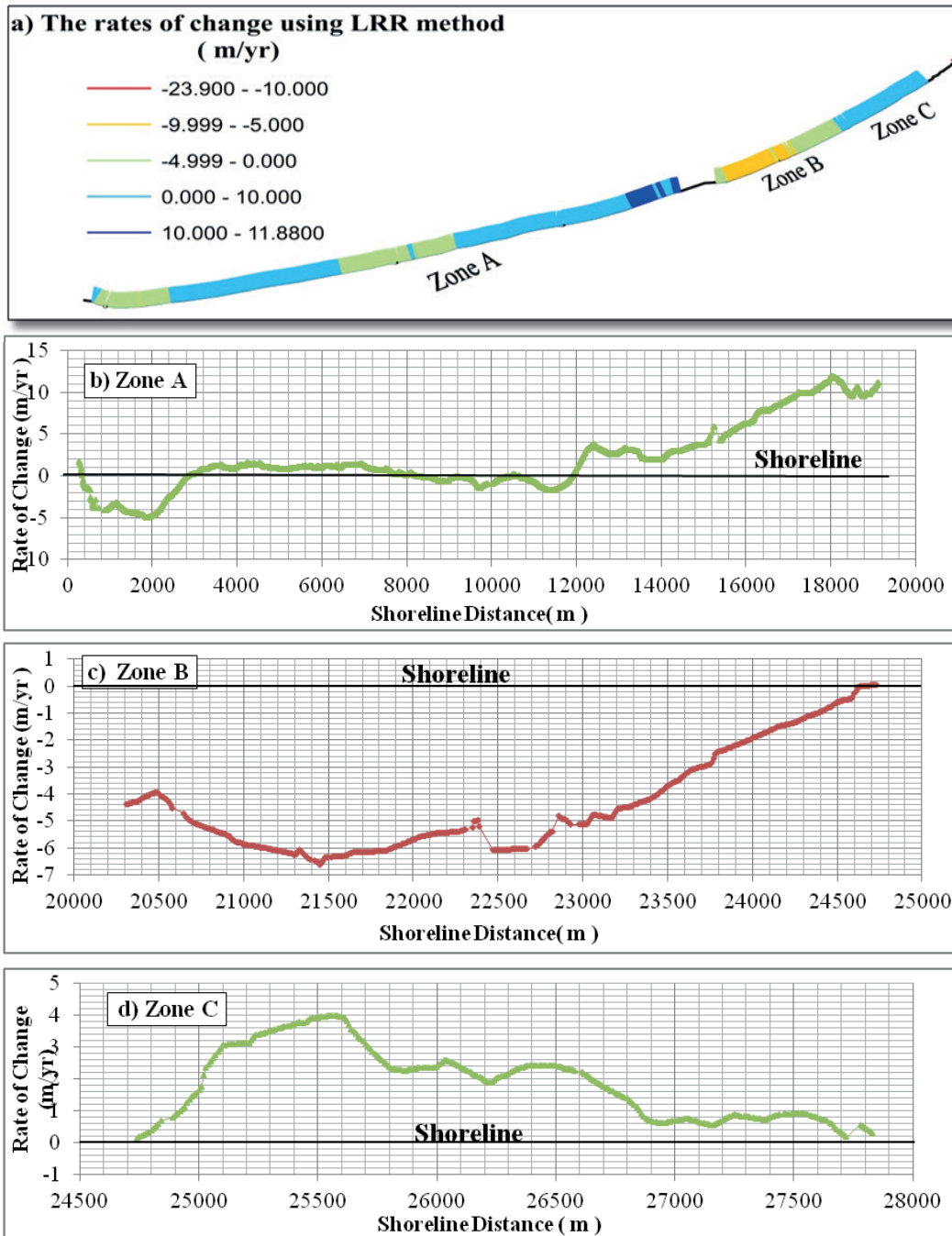


Figure 11. a) Statistical results using LRR method for the study area during (1995 - 2018), b) Rates of shoreline change for Zone A, c) Rates of shoreline change for Zone B, d) Rates of shoreline change for Zone C.

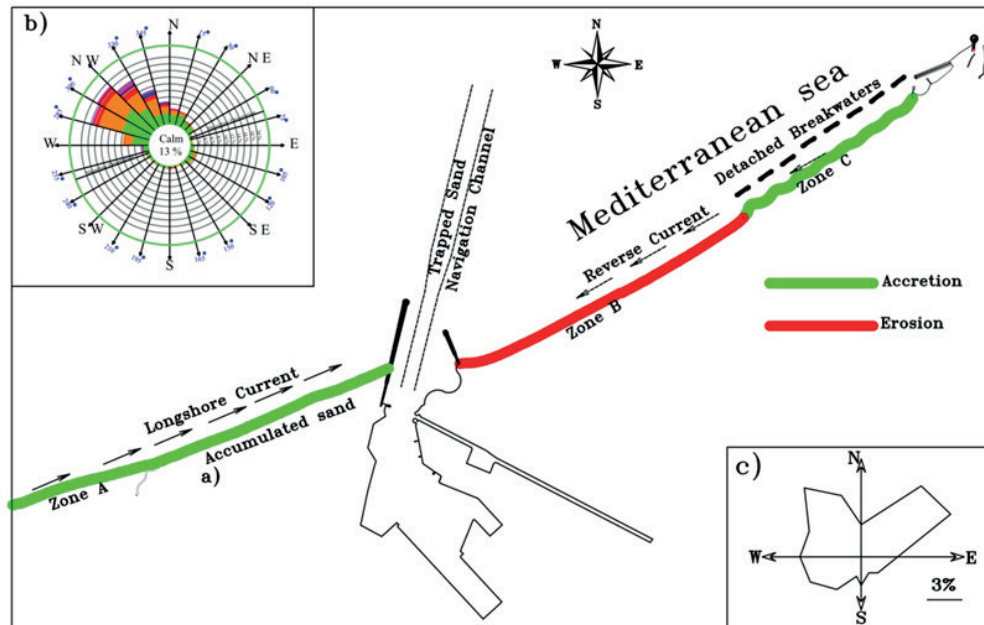


Figure 12. a) Erosion/accretion pattern of the study area, b) Wave rose at Damietta harbour, c) Current rose recorded at Damietta harbour.

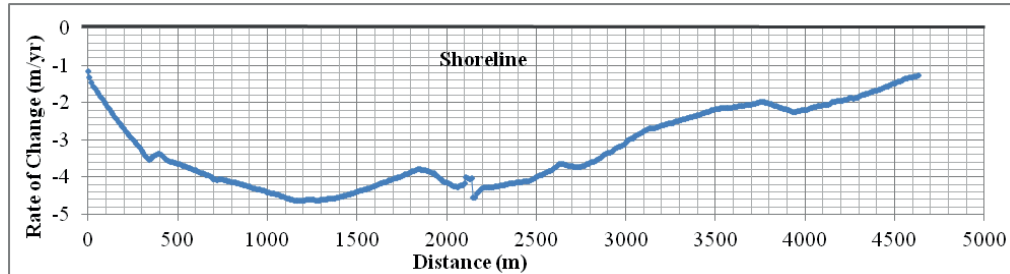


Figure 13. Average rates of shoreline change at zone B.

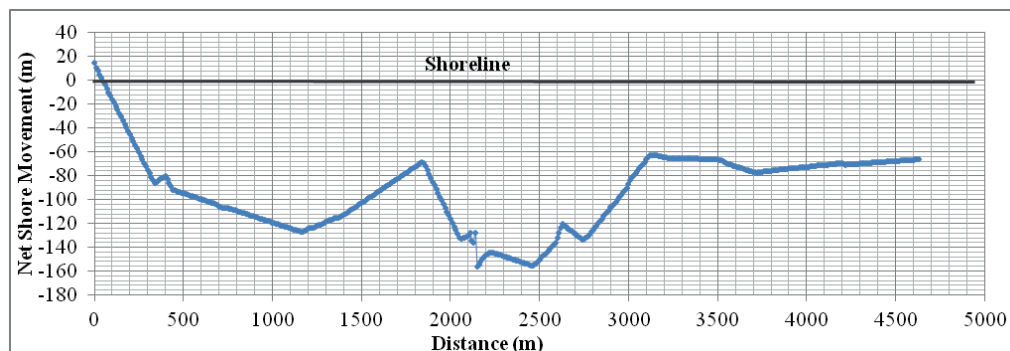


Figure 14. Net shore movement at zone B.

The erosion rate of this zone was a result of blockage of sediment discharge from both the western side and the eastern side. The western breakwater and the navigation channel trapped sediments from Burullus, and detached breakwaters at Ras El-Bar beach settle down any incoming sediment from Damietta promontory. So, zone B is considered one of the main hazard areas along the Northeastern shoreline of Nile delta and needs a sustainable solution. Sand nourishment is the solution current used in the eastern coast (Figure 15) to restore eroded area of the beach and to keep it available for recreation uses. However, it is a conventional solution that has rising periodic cost. Satellite image of 2019 shows four small groins that were constructed by Egyptian authorities in the first part of zone B. However, groins will not be effective without continuous sand nourishment, since sediment flux is trapped in both sides.

4.4 Prediction of future shoreline evolution

Shoreline prediction was carried out for zone B to clarify its expected position in the future if there no sustainable solution for this area is applied. The prediction accuracy of shoreline position is based on the historical processes that could be determined by satellite images. Numerous methods have been adopted for future prediction of shoreline position or sea-level rise like non-linear mathematical models, and the simplest and useful ones are the End Point Rate (EPR) and the Linear Regression Rate (LRR) models, (Li *et. al.*, 2001). So, in this case the EPR model has been used to predict the future shoreline

positions. The position of the future shoreline for a certain date is predicted using the rate of shoreline movement, the time interval between predicted and observed shoreline which can be expressed as:

$$Y_{pre} = r_{EPR}X_{pre} + b \quad (1)$$

where Y_{pre} represents the predicted distance from the baseline in meters, X_{pre} the time interval between predicted and observed shoreline, r_{EPR} the rate of change given from DSAS for each transect and b the Y-intercept given by,

$$r_{EPR} = (Y_n - Y_0) / (X_n - X_0) \quad (2)$$

$$b = Y_n - m_{EPR} \times X_n = Y_0 - m_{EPR} \times X_0 \quad (3)$$

where Y_n represents the predicted distance from the baseline in meters at the last shoreline date X_n and Y_0 the initial distance from the baseline in meters at the first shoreline date X_0 .

To validate this technique, shorelines of 1995 and 2010 and corresponding r_{EPR} were used to predict the shoreline of 2013. Root mean square error (RMSE) was calculated to evaluate the reliability of this method. The delineation between predicted values and actual values varied from 33.0 m to 0.02 with RMSE of 12.54 m and relative error of 0.63 m year⁻¹, that is considered a reasonable value for such a large shoreline.

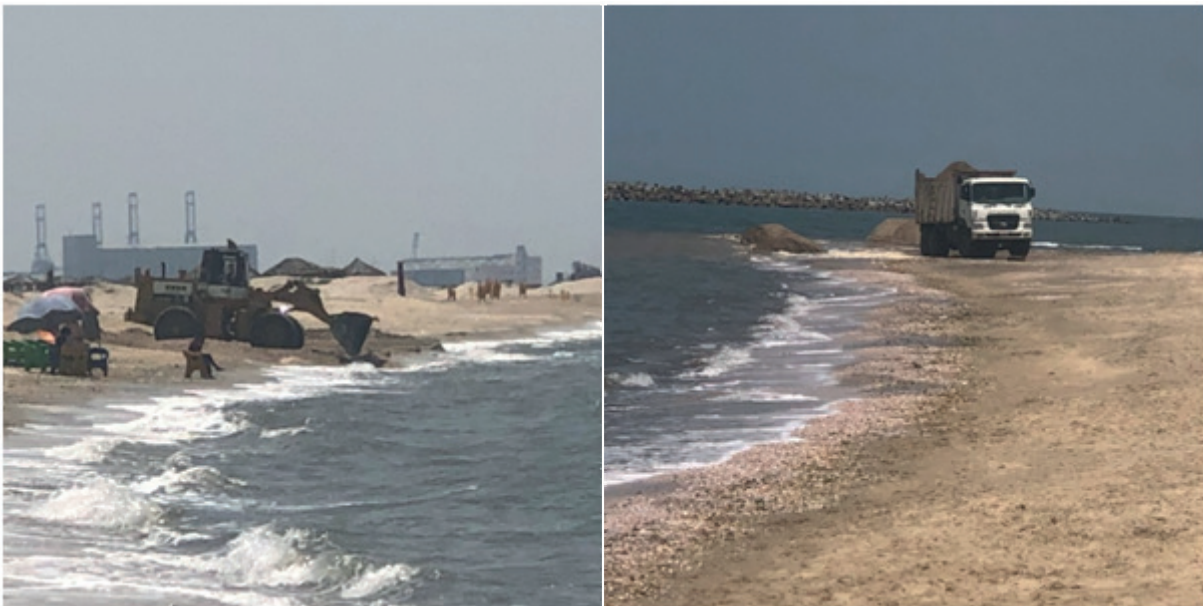


Figure 15. Sand nourishment in the eastern coast of Damietta harbour (April 2019).

To enhance prediction accuracy, the rate of change should be corrected as,

$$r_{\text{EPR}_{\text{corrected}}} = r_{\text{EPR}} + (\text{error} / \text{time interval}) \quad (4)$$

Shorelines of 2030, 2040, 2050 and 2060 were predicted after correction and shown in figure 16. From 2018 to 2060, the shoreline was estimated to retreat approximately 390.0 m in some points with an average regression of 280.0 m, which is considered a significant loss of area.

5. SUMMARY AND CONCLUSIONS

Remote sensing techniques were used to evaluate the impact of the Damietta harbour and its deep navigation channel on adjacent shorelines. DSAS was used to determine the accurate rate of change and predict the future shoreline evolution. The Damietta harbor and navigation channel have a deep impact on neighboring beaches as the navigation channel acts as a sediment trap that interrupts the long-shore transported sediment. The western breakwater prevents sediment movement partially from west to east, so the accretion zone is created on the western side of the harbour with accretion rate of 2.13 m year⁻¹. Hence, shoreline monitoring deduced that the eastern shoreline had an average erosion rate of -3.1 m year⁻¹ and it is considered a fatal hazard area along Northeastern shoreline of Nile Delta. Shoreline retreated from 1978 to 2018 by 156.3 m in some points and 92 m on average. Shoreline prediction shows that

shoreline will retreat by 390.0 m in some points with an average regression of 280.0 m in 2060 if no sustainable solution for this area is applied.

ACKNOWLEDGEMENT

The authors would like to thank the Hydraulic Research Institute (HRI), Egypt, for the invaluable help with the field data and assistance.

REFERENCES

- Abo Zed, A. B. (2007). Effect of waves and current on the siltation problem of Damietta harbour, Nile Delta coast, Egypt. *Mediterranean Coastal Engineering*, 8(2), 33-48. <https://doi.org/10.12681/mms.152>.
- Alesheikh, A. A., Ghorbanali, A., Nouri, N. (2007). Coastline change detection using remote sensing. *International Journal of Environmental Science & Technology*, 4(1), 61-66. <https://doi.org/10.1007/bf03325962>.
- Bahgat, M. (2018). Mitigation measures for sediment deposition problem inside the approach navigation channel of Damietta harbour. Hydraulic Research Institute report, July 2018, 1-49.
- Da Silveira, L. F., Benedet, L., Signorin, M., Bonanata, R. (2012). Evaluation of the relationships between navigation channel dredging and erosion of adjacent beaches in southern Brazil. *Coastal Engineering Proceedings*, 1(33), 106. <https://doi.org/10.9753/icce.v33.sediment.106>.

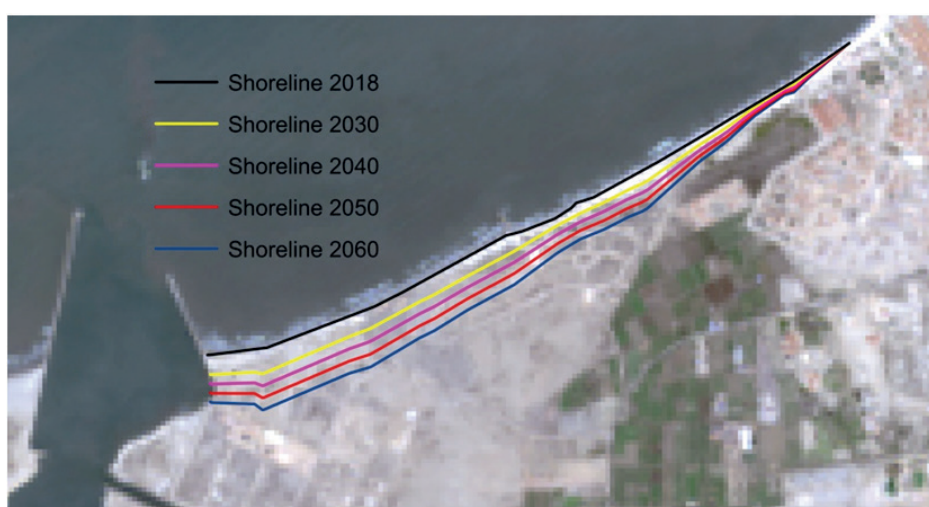


Figure 16. The predicted shoreline evolution of zone B.

- Danforth, W. W., Thieler, E. R. (1992). Digital Shoreline Analysis System (DSAS) user's guide; version 1.0 (No. 92-355). US Geological Survey. <https://doi.org/10.3133/ofr92355>.
- Deabes, E. (2010). Sedimentation processes at the navigation channel of Liquid Natural Gas (LNG), Nile Delta, Egypt. *International Journal of Geosciences*, 1(01), 14-20. <https://doi.org/10.4236/ijg.2010.11002>.
- Deguchi, I., Sawaragi, T., Ono, M., Koontanakulvong, S. (1994). Mechanism and estimation of sediment in Bangkok Bar Channel. *Coastal Engineering* 1995, 3002- 3015. <https://doi.org/10.1061/9780784400890.217>.
- Dewidar, K. H., Frihy, O. (2007). Pre-and post-beach response to engineering hard structures using Landsat time-series at the northwestern part of the Nile delta, Egypt. *Journal of Coastal Conservation*, 11(2), 133-142. <https://doi.org/10.1007/s11852-008-0013-z>.
- Dewidar, K. M., Frihy O.E. (2010). Automated Techniques for Quantification of Beach change Rates Using Landsat Series along the North-eastern Nile Delta, Egypt. *Journal of oceanography and marine science*, Vol. 1(2), 028-039.
- Do, A. T., Vries, S. D., Stive, M. J. (2019). The estimation and evaluation of shoreline locations, shoreline-change rates, and coastal volume changes derived from Landsat images. *Journal of Coastal Research*, 35(1), 56-71. <https://doi.org/10.2112/JCOASTRES-D-18-00021.1>.
- El Asmar, H.M. White, K. (2002). Changes in coastal sediment transport processes due to construction of new Damietta harbour, Nile Delta, Egypt. *Coastal Engineering*, 46(2), 127-138. [https://doi.org/10.1016/s0378-3839\(02\)00068-6](https://doi.org/10.1016/s0378-3839(02)00068-6).
- El Asmar, H. M., Taha, M. M., El-Sorogy, A. S. (2016). Morphodynamic changes as an impact of human intervention at the Ras El-Bar-Damietta harbor coast, NW Damietta promontory, Nile Delta, Egypt. *Journal of African Earth Sciences*, 124, 323-339. <https://doi.org/10.1016/j.jafrearsci.2016.09.035>.
- El Banna, M. M., Hereher, M. E. (2009). Detecting temporal shoreline changes and erosion/accretion rates, using remote sensing, and their associated sediment characteristics along the coast of North Sinai, Egypt. *Environmental Geology*, 58(7), 1419- 1427. <https://doi.org/10.1007/s00254-008-1644-y>.
- El nabwy, M. T., Elbeltagi, E., El Banna, M. M., Elshikh, M. M., Motawa, I., & Kaloop, M. R. (2020). An Approach Based on Landsat Images for Shoreline Monitoring to Support Integrated Coastal Management—A Case Study, Ezbet Elborg, Nile Delta, Egypt. *ISPRS International Journal of Geo-Information*, 9(4), 199. <https://doi.org/10.3390/ijgi9040199>
- El-Sharnouby, B. A., El-Alfy, K. S., Rageh, O. S., El-Sharabasy, M. M. (2015). Coastal changes along Gamasa beach, Egypt. *Journal of Coastal Zone Management*, 12, 393. <https://doi.org/10.4172/2473-3350.1000393>.
- Frihy, O. E., Deabes, E.A., Helmy, E. (2016). Compatibility analysis of dredged sediments from routine pathways and maintenance of harbor's channels for reuse in nearshore nourishment in the Nile Delta, Egypt. *Journal of Coastal Research*, 32(3), 555-566. <https://doi.org/10.2112/jcoastres-d-14-00181.1>.
- Frihy, O. E., Komar, P. D. (1993). Long-term shoreline changes and the concentration of heavy minerals in beach sands of the Nile Delta, Egypt. *Marine Geology*, 115(3-4), 253-261. [https://doi.org/10.1016/0025-3227\(93\)90054-y](https://doi.org/10.1016/0025-3227(93)90054-y).
- Frihy, O.E., El Banna, M. M. El Kolfat, A. I. (2004). Environmental impacts of Baltim and Ras El Bar shore-parallel breakwater systems on the Nile Delta littoral zone, Egypt. *Environmental Geology*, 45(3), 381-390. <https://doi.org/10.1007/s00254-003-0886-y>.
- Gad, M. A., Saad A., El-Fiky, A., Khaled, M. (2013). Hydrodynamic modeling of sedimentation in the navigation channel of Damietta harbor in Egypt. *Coastal Engineering Journal*, 55(2), 1-31. <https://doi.org/10.1142/s0578563413500071>.
- Guariglia, A., Buonamassa, A., Losurdo, A., Saladino, R., Trivigno, M. L., Zaccagnino, A., Colangelo, A. (2006). A multisource approach for coastline mapping and identification of shoreline changes. *Annals of geophysics*, 49(1).
- Kabir, M. A., Salaudiddin, M., Hossain, K. T., Tanim, I. A., Saddam, M. M. H., Ahmad, A. U. (2020). Assessing the shoreline dynamics of Hatiya Island of Meghna estuary in Bangladesh using multiband satellite imageries and hydro-meteorological data. *Regional Studies in Marine Science*, 35, 101167. <https://doi.org/10.1016/j.rsma.2020.101167>.
- Khalifa, A. M. (2017). Controlling sedimentation problems of Damietta harbor navigation channel using numerical modelling. M.Sc. Thesis, Alexandria University faculty of engineering, Alexandria, 1-150.
- Khalifa, A. M., Soliman, M. R., Yassin, A. A. (2017). Assessment of a combination between hard structures and sand nourishment eastern of Damietta harbor using numerical modeling. *Alexandria Engineering Journal*, 56(4), 545-555. <https://doi.org/10.1016/j.aej.2017.04.009>.
- Kuleli, T. (2010). Quantitative analysis of shoreline changes at the Mediterranean Coast in Turkey. *Environmental monitoring and assessment*, 167(1-4), 387-397. DOI: 10.1007/s10661-009-1057-8.
- Kumar, A., Narayana, A. C., Jayappa, K. S. (2010). Shoreline changes and morphology of spits along southern Karnataka, west coast of India: A remote sensing and statistics-based approach. *Geomorphology*, 120(3-4), 133-152. <https://doi.org/10.1016/j.geomorph.2010.02.023>.
- Louati, M., Saïdi, H., Zargouni, F. (2015). Shoreline change assessment using remote sensing and GIS techniques: a case study of the Medjerda delta coast, Tunisia. *Arabian Journal of Geosciences*, 8(6), 4239-4255. DOI: 10.1007/s12517-014-1472-1.

- Leys, V., Ryan P. Mulligan, R.P. 2011. Modelling coastal sediment transport for harbour Planning: Selected case studies. *Sediment Transport*, 31. <https://doi.org/10.5772/15007>.
- Li, R., Liu, J.K., Felus, Y. (2001). Spatial modeling and analysis for shoreline change detection and coastal erosion monitoring. *Marine Geodesy*, 24(1), 1-12. <https://doi.org/10.1080/01490410151079891>
- Moore, L. J. (2000). Shoreline mapping techniques. *Journal of coastal research*, 111-124.
- Nguyen, V. T., Zheng, J. H., Zhang, J. S. (2013). Mechanism of back siltation in navigation channel in Dinh an estuary, Vietnam. *Water Science and Engineering*, 6(2), 178-188. <https://doi.org/10.3882/j.issn.1674-2370.2013.02.006>.
- Niya, A. K., Alesheikh, A. A., Soltanpor, M., Kheirkhazarkesh, M. M. (2013). Shoreline change mapping using remote sensing and GIS. *International Journal of Remote Sensing Applications*, 3(3), 102.
- Perillo G. M., Cuadrado D. (1991). Geomorphologic evolution of E1 Toro channel, Bahia Blanca Estuary (Argentina) prior to dredging. *Marine Geology*, 97(3-4), 405-412. [https://doi.org/10.1016/0025-3227\(91\)90129-R](https://doi.org/10.1016/0025-3227(91)90129-R).
- Sanga, I.P.L., Dubi, A.M. (2004). Impact of improvement of entrance channel on the rate of sediment deposition into the Dar es Salam harbour. *Western Indian Ocean J. Mar. Sci.*, 3(2), 105-112. <https://doi.org/10.4314/wiojms.v3i2.28454>.
- Wang, X., Liu, Y., Ling, F., Liu, Y., Fang, F. (2017). Spatio-Temporal change detection of Ningbo coastline using Landsat time-series images during 1976–2015. *ISPRS International Journal of Geo-Information*, 6(3), 68. DOI:10.3390/ijgi6030068.
- Zimmermann, N., Trouw, K., Wang, L., Mathys, M., Delgado, R., Verwaest, T. (2012). Longshore transport and sedimentation in a navigation channel at Blankenberge (BELGIUM). *Coastal Engineering*, 1(33), 111. <https://doi.org/10.9753/icce.v33.sediment.111>.

